

Microcalcifications Detection using Image Processing

Joel Quintanilla-Domínguez¹, José Ruiz-Pinales², José Miguel Barrón-Adame³,
Rafael Guzmán-Cabrera²

¹ Universidad Politécnica de Juventino Rosas,
Mexico

² Universidad de Guanajuato División de Ingenierías Campus Irapuato-Salamanca,
Mexico

³ Universidad Tecnológica del Suroeste de Guanajuato,
Departamento de Tecnologías de la Información y Comunicación,
Mexico

joel_quintanilla79@yahoo.com.mx, pinales@ugto.mx, mbarrona@hotmail.com, guzman@ugto.mx

Abstract. Breast cancer is the most common cause of death in women and the second leading cause of cancer deaths worldwide. Primary prevention in the early stages of the disease becomes complex as the causes remain almost unknown. However, some typical signatures of this disease, such as masses and microcalcifications appearing on mammograms, can be used to improve early diagnostic techniques, which is critical for women's quality of life. X-ray mammography is the main test used for screening and early diagnosis, and its analysis and processing are the keys to improving breast cancer prognosis. In this work, an effective methodology to detect microcalcifications in digitized mammograms is presented. This methodology is based on the synergy of image processing, pattern recognition and artificial intelligence. The methodology consists in four stages: image selection, image enhancement and feature extraction based on mathematical morphology operations applying coordinate logic filters, image segmentation based on partitioning clustering methods such as k-means and self organizing maps and finally a classifier such as an artificial metaplasticity multilayer perceptron. The proposed system constitutes a promising approach for the detection of Microcalcifications. The experimental results show that the proposed methodology can locate Microcalcifications in an efficient way. The best values obtained in the experimental results are: accuracy 99.93% and specificity 99.95%, These results are very competitive with those reported in the state of the art.

Keywords. Microcalcifications, image processing, breast cancer.

1 Introduction

Breast cancer is one of the most dangerous types of cancer among women around the world. It is also one of the leading causes of mortality in middle and old aged women. The World Health Organization's International Agency for Research on Cancer estimates that more than 1 million cases of breast cancer will occur worldwide annually, with 580,000 cases occurring in developed countries and the remainder in developing countries. The risk of a woman developing breast cancer during her life time is approximately 11% [1]. The early detection of breast cancer is of vital importance for the success of treatment, with the main goal to increase the probability of survival for patients. Currently the most reliable and practical method for early detection and screening of breast cancer is mammography. Microcalcifications can be an important early sign of breast cancer, these appear as bright spots of calcium deposits. Individual microcalcifications are sometimes difficult to detect because of the surrounding breast tissue, their variation in shape, orientation, brightness and diameter size [2]. Microcalcifications are potential primary indicators of malignant types of breast cancer, therefore their detection can be important to prevent and treat the disease. In this paper, an effective methodology in order to detect Microcalcifications in digitized mammograms is presented. This approach is based on the synergy

of Image Processing, Pattern Recognition and Artificial Intelligence. But it is still a hard task to detect all the Microcalcifications in mammograms, because of the poor contrast with the tissue that surrounds them.

However, many techniques have been proposed to detect the presence of microcalcifications in mammograms: image enhancement techniques, Artificial Neural Networks, wavelet analysis, Support Vector Machines, mathematical morphology, image analysis models, fuzzy logic techniques, etc. Image enhancement algorithms have been utilized for the improvement of contrast features and the suppression of noise. In [3] proposed five image enhancement algorithms for the detection of microcalcifications in mammograms.

Bhattacharya and Das [4], proposed a method based on discrete wavelet transform due to its multiresolution properties with the goal to segment microcalcifications in digital mammograms. Morphological Top-Hat algorithm was applied for contrast enhancement of the microcalcifications. Fuzzy C-Means clustering algorithm was implemented for intensity-based segmentation. Sung et al. [5], proposed an approach by means of mathematical morphology operations and wavelet transform to locate the microcalcifications in digital mammogram.

In [6] proposed an algorithm that was tested over several images taken from the digital database for screening mammography for cancer research and diagnosis, and it was found to be absolutely suitable to distinguish masses and microcalcifications from the background tissue using morphological operators and then extract them through machine learning techniques and a clustering algorithm for intensity-based segmentation. Segmentation processes for the detection of textures, ROIs, lesions, tumors have also been used on photo-acoustic images [7] and thermographic images [8].

The remaining sections of this work are organized as follows: Section 2, presents the details of the proposed method. Section 3, presents the details of the proposed method and experimental results while the conclusions are presented in sections 4, respectively.

2 Methodology

2.1 Image Selection

The images used to train and test this methodology were extracted from the mini-mammographic database provided by the Mammographic Image Analysis Society, MIAS [17]. Each mammogram from the database is 1024×1024 pixels and with a spatial resolution of 200 micron pixel edge. These mammograms have been reviewed by an expert radiologist and all the abnormalities have been identified and classified. The place where these abnormalities such as Microcalcifications, have been located is known as, Region of Interest (ROI). The ROI size in this work is 256×256 pixels.

2.2 ROI Enhancement

The difficulty for the detection of Microcalcifications depends on some factors, such as, size, shape and distribution with respect to their morphology. On the other hand the Microcalcifications are often located in a non-homogeneous background and due to their low contrast with the background, its intensity may be similar to noise or other structures [9-10]. In this paper, the goal of image enhancement is to improve the contrast between the Microcalcifications clusters and background, for achieving this task morphological operations based on Coordinate Logic Filters (CLF) are implemented.

Mathematical Morphology is a discipline in the field of image processing which involves an analysis of the structure of images. The geometrical structure of image is determined by locally comparing it with a predefined elementary set called structuring element. Image processing using morphological transformations is a process of information removal based on size and shape, in this process irrelevant image content is eliminated selectively, thus the essential image features can be enhanced. Morphological operations are based on the relationships between the two sets: an input image, G , and a processing operator, the structuring element, SE , which is usually much smaller than the input image. By selecting the shape and size of structuring element, different results may be obtained in the

output image. The fundamental morphological operations are: erosion and dilation.

CLF were proposed in [11], and constitute a class of non-linear digital filters that are based on the application of Coordinate Logic Operations (CLO) to a single image as dictated by a SE, where CLO are the basic logic operations (NOT, AND, OR, and XOR, and their combinations). CLF are very efficient in digital signal processing applications, such as noise removal, magnification, skeletonization, coding, edge detection, feature extraction, fractal modelling and can execute the morphological operations (erosion, dilation, opening and closing) and the successive filtering and managing of the residues. The execution of CLO (AND, OR) in CLF is performed on the binary values of the image pixels and are analogous to the execution of (MIN, MAX) in the morphological filters. That makes the CLF have analogous operability with the corresponding morphological ones. Moreover, CLF satisfy all the corresponding morphological properties except the increasing property. The CLF coincide with morphological filters in the case of binary images. They could also coincide with gray-scale morphological filters provided that images are quantized and mapped on a specific set of decimal values [5]. Given a gray level image G, the decomposition in a set of binary images $S_k, k=0,1,\dots,n-1$, according to the decomposition of the (i,j) pixel, is denoted by:

$$g = \sum_{k=0}^{n-1} S_k(i,j)2^k, \quad i = 1,2, \dots, M, \quad j = 1,2, \dots, N, \quad (1)$$

where $S_k(i,j), k = 0,1, \dots, n - 1$ are binary components of the decimal pixel values $g(i,j), i=1,2,\dots,M, j=1,2,\dots,N$, according to equation 1, the Coordinate Logic Dilation (CLD, \oplus) and Coordinate Logic Erosion (CLE, \ominus) of the image G by the structuring element SE, are defined by following equations:

$$CLD = COR \ g(i,j) \in SE = \sum_{k=0}^{n-1} (S_k(i,j))_{SE}^D 2^k, \quad (2)$$

$$i = 1,2, \dots, M, \quad j = 1,2, \dots, N,$$

$$CLE = CAND \ g(i,j) \in SE = \sum_{k=0}^{n-1} (S_k(i,j))_{SE}^D 2^k, \quad (3)$$

$$i = 1,2, \dots, M, \quad j = 1,2, \dots, N.$$

The contrast can be defined as the difference in intensity between an image structure and its background. By combining morphological operations, several image processing tasks can be performed, but in this work morphological operations are used to achieve contrast enhancement. In [12], the contrast enhancement technique using mathematical morphology is called morphological contrast enhancement. Morphological contrast enhancement is based on morphological operations known as top-hat and bottom-hat transforms. A Top-Hat is a residual filter which preserves those features in an image that can fit inside the structuring element and removes those that cannot in other words the Top-Hat transform is used to segment objects that differ in brightness from the surrounding background in images with uneven background intensity. The Top-Hat transform is defined by the following equation:

$$G_T = G - [(G \ominus SE) \oplus SE], \quad (4)$$

where G is the input image, G_T is the transformed image, SE is the structuring element, \ominus represents morphological erosion operation, \oplus represents morphological dilation operation and - image subtraction operation. $[(G \ominus SE) \oplus SE]$ is also known as the morphological opening operation.

2.3 Image Segmentation by Clustering Algorithms

Image segmentation is an important task in the field of image processing and computer vision and involves identifying objects or regions with the same features in an image. The purpose of image segmentation is to subdivide an image into non-overlapping, constituent regions which are homogeneous with respect to some features such as gray level intensity or texture. The level to which the subdivision is carried out depends on the problem being solved [13]. In the field of medical

imaging, segmentation plays an important role because it facilitates the delineation of anatomical structures and other regions of interest. For the specific case as Microcalcifications detection, several works based on image segmentation by means of clustering algorithms have been proposed [14-16]. In this work, for the image segmentation stage, two techniques based on partitioning clustering algorithms are used. The aim of this stage is to segment the ROI images to make easier the Microcalcifications detection. The algorithms used in this stage are k-means and SOM.

k-means is one of the simplest unsupervised learning algorithms that solve the well known clustering problem. The procedure follows a simple and easy way to classify a given data set Z in a d -dimensional space, through a certain number of clusters (assume k clusters) fixed a priori. The main idea is to define k prototypes, one for each cluster. The next step is to take each point belonging to a given Z and associate it to the nearest prototype. When no point is pending, the first step is completed and an early group is done. At this point is necessary to re-calculate k new prototypes as barycenters of the clusters resulting from the previous step. Then to obtain these k new prototypes, a new binding has to be done between the same data set points and the nearest new prototype. A loop has been generated. As a result of this loop we may notice that the k prototypes change their location step by step until no more changes are done. In other words, prototypes do not move any more. Finally, this algorithm aims at minimizing an objective function (5), in this case a squared error function:

$$J = \sum_{j=1}^k \sum_{i=1}^n \|z_i^{(j)} - v_j\|^2, \quad (5)$$

where $\|z_i^{(j)} - v_j\|^2$ is chosen distance measure between a data point $z_i^{(j)}$ and the cluster v_j is an indicator of the distance of the data points from their cluster prototypes. SOM neural networks, introduced by [10], are simple analogues to the brain's way to organize information in a logical manner. The main purpose of this neural information processing is the transformation of a

feature vector of arbitrary dimension drawn from the given feature space into simplified generally two-dimensional discrete maps. This type of neural network utilizes an unsupervised learning method, known as competitive learning, and is useful for analyzing data with unknown relationships. The basic SOM Neural Network consists of an input layer, and an output (Kohonen) layer which is fully connected with the input layer by the adjusted weights (prototype vectors). The number of units in the input layer corresponds to the dimension of the data. The number of units in the output layer is the number of reference vectors in the data space. There are several steps in the application of the algorithm. These are competition and learning, to get the winner in the process. In the training (learning) phase, the SOM forms an elastic net that folds onto the "cloud" formed by the input data. Similar input vectors should be mapped close together on nearby neurons, and group them into clusters. If a single neuron in the Kohonen layer is excited by some stimulus, neurons in the surrounding area are also excited. That means for the given task of interpreting multidimensional image data, each feature vector $\dagger x$, which is presented to the four neurons of the input layer, typically causes a localized region of active neurons against the quiet background in the Kohonen layer. The degree of lateral interaction between a stimulated neuron j (x) and neighbouring neurons is usually described by a Gaussian function:

$$h_{k,j}(\vec{x}) = \exp\left(-\frac{d_{k,j}^2(\vec{x})}{2\sigma^2}\right), \quad (6)$$

where d is the lateral neuron distance in the Kohonen layer, σ is the *effective width* that changes during the learning process, and h is the activity of the neighbouring neurons. Feature vectors occur in the Kohonen layer in the same topological order as they are presented by the metric (similarity) relations in the original feature space, while performing a dimensionality reduction of the original feature space. Before the self-organizing procedure begins, the link values, called weights. \vec{w}_k connects the n input layer neurons to the l neurons in the Kohonen layer. n is the dimension of the input space (Microcalcifications feature space), and l is the

number of all Kohonen neurons with $k = 1, 2, \dots, m, \dots, l$.

The neurons of the Kohonen layer compete to see which neuron will be stimulated by the feature vector \vec{x} . The weights \vec{w}_k are used to determine only one stimulated neuron in the Kohonen layer after the *winner-takes-all* principle. This principle can be summarized as follows: for each \vec{x} , the Kohonen neurons compute their respective values of a discriminant function (i.e., Euclidean distance $\|\vec{x}_j - \vec{w}_k\|$). These values are used to define the winner neuron. That means the network determines the index j of that neuron, whose weight \vec{w}_k is the closest to vector \vec{x}_i by:

$$j(\vec{x}_i) = \underset{k}{\operatorname{argmin}} \|\vec{x}_i - \vec{w}_k\|, \quad k = 1, 2, \dots, m, \dots, l. \quad (7)$$

The neighbourhood function or Gaussian function determines how much the neighbouring neurons become modified. Neurons within the winners neighbourhood participate in the learning process. During the self-organizing process, the neighbourhood size decreases until its size σ is zero. In this case, only the winning neuron is modified each time an input vector is presented to the network. The learning rate η – the amount each weight can be modified – decreases during the learning as well. Once the SOM algorithm has converged, two-dimensional feature maps of Kohonen neurons display the following important statistical characteristics of the represented feature space [10].

2.4 Classification of Microcalcifications by AMMLPs

Artificial Neural Networks (ANNs) are used in a wide variety of data processing applications where real-time data analysis and information extraction are required. One advantage of the ARTIFICIAL NEURAL NETWORKS approach is that most of the intense computation takes place during the training process. Once ANNs are trained for a particular task, their operation is relatively fast and unknown samples can be rapidly identified in the field.

In this work, Artificial Metaplasticity (AMP) is applied to the learning algorithm of a Multi-Layer

Perceptron. Metaplasticity is a biological concept related to the way information is stored by synapses in the brain. Artificial metaplasticity was recently proposed in [17], where it is modelled by giving more importance to less frequent patterns in the training process. One advantage of the use of AMP is that it usually results in a more efficient training because a small set of training patterns is usually required. This approach is in fact equivalent to the application of importance sampling to artificial neural networks training [18].

In the classic backpropagation algorithm the learning rate is usually fixed for all input patterns meaning that it gives the same importance to all patterns. AMP can be included in the training process by simply introducing a weighting function $1/f_x^*(x)$ in the weight update equation of the learning algorithm [19]. As a matter of fact, the learning rate of the backpropagation algorithm is replaced by a variable learning rate $\eta(x) = \eta/f_x^*(x)$ which is a function of the input vector x :

$$\Delta W^s = -\eta(x) \frac{\partial E}{\partial W^s}. \quad (8)$$

Ideally, the function $f_x^*(x)$ must be a proper approximation of the probability density function of the input patterns. So, less frequent patterns are given a larger learning rate than more frequent ones do. In practice, a suitable function must be chosen in order to improve learning. Neural networks are able to approximate Bayesian posterior class probabilities provided there is sufficient training data and the network has one output for each class [20-21]. This implies that the posterior probabilities obtained by the neural network can be used. However, suitable posterior probabilities are only available after proper training of the neural network. In this paper, the following function is used:

$$f_x^*(x) = \frac{A}{\sqrt{(2\pi)^N e^{B \sum_{i=1}^N x_i^2}}}, \quad (9)$$

where N is the dimension of the input vector X (for the second hidden layer, X is substituted by the output vector of the first hidden layer, and so on) and $A, B \in \mathbb{R}^+$ are empirically determined parameters. This function corresponds to the

assumption that the input patterns are normally distributed.

3 Results

The proposed methodology is applied to each of the ROI images individually in order to show the obtained results by means of a segmented image. Several ROI images with dense tissue and the presence of Microcalcifications were selected to train and test the proposed methodology. The morphological Top-Hat transform is used in order to enhance the ROI image, with the goal of detecting objects that differ in brightness from the surrounding background, in this case the goal is to increase the contrast between the Microcalcifications and the background. The size of each SE used is 3×3 .

In the next stage two window-based features such as, mean and standard deviation are extracted from enhanced images within a rectangular pixel window of size 5×5 . In this paper, each image obtained after applying the image enhancement process as well as the images obtained by window-based features, are considered as features to generate a set of patterns that represent Microcalcifications and normal tissue. Each pattern is constructed from the gray level intensity of pixels of the obtained images, representing each one a point in d-dimensional space. It is known that each image contains pixels belonging to Microcalcifications and to normal tissue, then each analyzed pattern belongs to one of two possible classes, i.e. there are patterns that belong to the set Q_1 if correspond to Microcalcifications and patterns belonging to normal tissue Q_0 .

Next, a Feature Vector (FV) for each ROI image is built, a set of FVs is formed for each obtained image from the previous process. First, a mapping is performed from the gray level intensity to a vector as follows: $f(x, y) \rightarrow x^{(q)} = \{x^q\}_{q=1 \dots M \times N}$ where, q is the index that corresponds to one pixel when the image is decomposed column by column, $f(x, y)$ is the gray level of the q-th pixel, (x, y) are the coordinates of each pixel in the image and Q is the set of all pixels of the ROI. If the ROI size is $M \times N$, then are obtained $M \times N$ vectors $x^{(q)}$ in the Q set. Then the FV can be built as $FV_s = \{x^{(qs)}: q_s =$

Table 1. Number of patterns assigned to Q1 an Q0

Label	Number of patterns by k-means	Number of patterns by SOM
Q0	588181	583081
Q1	1643	6743

$1 \dots, Q_s\}$, where $x^{(qs)} \in \mathbb{R}^d$ is a d-dimensional vector, and Q_s is the number of pixels of the image, where $x^{(qs)} = \{[x_1^{(qs)}, x_2^{(qs)}, x_3^{(qs)}, x_4^{(qs)}]\}$. Where, $x_1^{(qs)}$ corresponds to the gray level intensity of the original image, $x_2^{(qs)}$ corresponds to the gray level of the enhanced image, $x_3^{(qs)}$ and $x_4^{(qs)}$ correspond to the mean and standard deviation of the enhanced images, respectively. The set of FVs is then clustered using two different clustering methods and obtaining the corresponding labels for each class, where only one cluster corresponds to MC and the rest of the clusters correspond to normal tissue.

In this work, criterions were used to determine which cluster represents an MC group: minimum number of data clustered into class with maximum gray level value as well as the clusters separability approach. A between-class dispersion matrix S_b and an intra-class dispersion matrix S_w are used. S_b represents the dispersion around the mean of the mixture of clusters and S_w represents the dispersion of the cluster around its prototype. These matrices are used to obtain a separability metric between clusters as proposed in [22]. The obtained results of clustering are represented as a segmented image in several regions that depend on the number on clusters, the final form of presenting our results is through a binary image that is, with ones corresponding to the label of Microcalcifications and with zeros corresponding to the label of the union of the remaining clusters, that we consider as non-Microcalcifications or normal tissue.

The initial conditions for the segmentation and results for each clustering method are presented next. For k-means: the number of clusters takes values from 2 to 6, cluster centers are initialized randomly, Euclidean distance is used and the maximum number of iterations is 100.

Table 2. Results of balancing

Label	Number of patterns by k-means	Number of patterns by SOM
Q0	8215	33715
Q1	1643	6743

Table 3. Number of patterns used for training and testing

	$Q_{1/0}$	Number of Samples		Total
		Training	Testing	
k-means	Q_1	1160	483	1643
	Q_0	5741	2474	8215
SOM	Q_1	5413	1330	6743
	Q_0	26954	6761	33715

Table 4. The best neural network structures and metaplasticity parameters

Data Set FV_s	Neural Network Structure			Metaplasticity Parameters		Mean Squared Error
	I	HL	O	A	B	
k-means	4	15	1	39	0.5	0.01
	4	12	1	39	0.5	0.01
SOM	4	15	1	39	0.25	0.01
	4	10	1	39	0.5	0.01

Table 5. Confusion matrices and performance of the classifiers

AMMLP Structure	Desired Results	MC	Output Results Normal Tissue	Sensitivity (%)	Specificity (%)	Accuracy (%)
k-means						
4:15:1	MC	483	0	100	99.67	99.72
	Normal Tissue	8	2466			
4:12:1	MC	476	7	98.55	99.63	99.45
	Normal Tissue	9	2465			
SOM						
4:15:1	MC	1328	2	99.84	99.95	99.93
	Normal Tissue	3	6758			
4:10:1	MC	1317	13	99.02	99.94	99.78
	Normal Tissue	4	6757			

The initial conditions for the SOM are: the network structure is $[4 k]$, where k takes values from 2 to 16, the weights are initialized randomly, the topology function is an hexagonal layer, Euclidean distance is used and the maximum epoch is 100.

Table 1 shows the number of patterns assigned to classes Q_0 and Q_1 from the obtained results in

the clustering stage by k-means and SOM respectively.

Due to the large amount of patterns that do not belong to Microcalcifications with respect to the number of patterns that belong to Microcalcifications a balancing was performed, see Table 2.

To comparatively evaluate the performance of the classifiers, all the classifiers presented in this

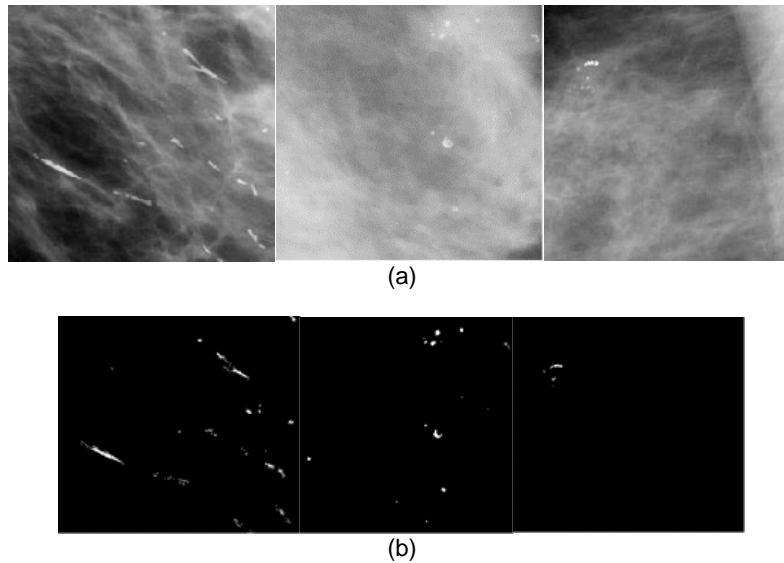


Fig. 1. Microcalcification detection by the proposed methodology. (a) Original ROIs. (b) 3rd partition. (c) 4th partition (d) 6th partition

particular case were trained with the same training dataset and tested on the same testing dataset. In order to determine the neural network structure and metaplasticity parameters, the same network parameters as applied in [23] and [17], were used. Table 4 shows the metaplasticity parameters A and B and the best network structures. Patterns extracted from the set of FVs are used to train and test the classifiers. For this case 70% of the data were used for training and 30% for testing, see Table 3.

In our work different network structures were used; the activation function is a sigmoid; and with the same metaplasticity parameters. Table 4 shows the best network structure and metaplasticity parameters for each FV.

A confusion matrix is built to determine the probability of false detection. Table 5 shows the performance of the classifiers presented in this work as well as the corresponding confusion matrices. As it can be shown, the best accuracy (99.93%) and specificity (99.95%) are obtained for a SOM and an AMMLP with a [4:15:1] structure. The second best accuracy (99.78%) and specificity (99.94%) are also obtained for a SOM and an AMMLP. However, the best sensitivity (100%) is obtained for k-means and an AMMLP with a [1:15:1] structure.

Finally, Figure 1 shows examples of the obtained results of the detection of Microcalcifications using the methodology proposed in this paper.

4 Conclusion

In this work a system for microcalcification detection was proposed based on two clustering algorithms, k-means and Self Organizing Maps, Coordinate Logic Filters and a neural network based on Artificial Metaplasticity. Clustering algorithms help us get a better comprehension and knowledge of the data with the objective of segmenting the image into different areas (background and MC). Before applying the clustering algorithms, we applied a digital image processing technique for image enhancement using mathematical morphology operations in order to improve the contrast between Microcalcifications and the background in the ROIs. One advantage of mathematical morphology operations based on Coordinate Logic Filters is due to their easy hardware implementation, although in this work only simulation was carried out. The AMMLP classifier plays an important role in our methodology because ARTIFICIAL NEURAL

NETWORKS can learn structure in data through examples contained in a training set and then can conduct complex decision making. From the obtained results, we conclude that the proposed system constitutes a promising approach for the detection of Microcalcifications. The experimental results show that the proposed methodology can locate Microcalcifications in an efficient way.

References

1. **Pal, N., Bhowmick, B., Patel, S., Pal, S., & Das, J. (2008).** A multi-stage neural network aided system for detection of microcalcifications in digitized mammograms. *Neurocomputing*, Vol. 71, No. 13-15, pp. 2625–2634. DOI:10.1016/j.neucom.2007.06.015.
2. **Wei, L., Yang, Y., & Nishikawa, R. (2009).** Microcalcification classification assisted by content-based image retrieval for breast cancer diagnosis. *Pattern Recognition*, Vol. 42, No. 6, pp. 1126–1132. DOI: 10.1016/j.patcog.2008.08.028.
3. **Papadopoulos, A., Fotiadis, D., & Costaridou, L. (2008).** Improvement of microcalcification cluster detection in mammography utilizing image enhancement techniques. *Computers in Biology and Medicine*, Vol. 38, No. 10, pp. 1045–1055. DOI: 10.1016/j.compbiomed.2008.07.006.
4. **Bhattacharya, M. & Das, A. (2007).** Fuzzy logic based segmentation of microcalcification in breast using digital mammograms considering multiresolution. *International Machine Vision and Image Processing Conference*, pp. 98–105. DOI: 10.1109/IMVIP.2007.33.
5. **Sung-Nien, Y., Kuan-Yuei, L., & Yu-Kun, H. (2006).** Detection of microcalcifications in digital mammograms using wavelet filter and markov random field model. *Computerized Medical Imaging and Graphics*, Vol. 30, No. 3, pp. 163–173. DOI: 10.1016/j.compmedimag.2006.03.002.
6. **Guzman-Cabrera, R., Guzman-Sepulveda, J., Torres-Cisneros, M., May-Arrijoja, D., Ruiz-Pinales, J., Ibarra-Manzano, O., Avina-Cervantes, G., & Gonzalez-Parada, A. (2013).** Digital image processing technique for breast cancer detection. *International Journal of Thermophysics*, Vol. 34, No. 8, pp. 1519–1531. DOI: 10.1007/s10765-012-1328-4.
7. **Guzman-Cabrera, R., Guzman-Sepulveda, J.R., Torres-Cisneros, M., May-Arrijoja, D., Ruiz-Pinales, J., Ibarra-Manzano, O., & Avina-Cervantes, G. (2013).** Pattern recognition in photoacoustic dataset. *International Journal of Thermophysics*, Vol. 34, No. 8-9, pp. 1638–1645. DOI: 10.1007/s10765-013-1452-9.
8. **Guzman-Cabrera, R., Guzman-Sepulveda, J., Gonzalez-Parada, A., Rosales-Garcia, J., Torres-Cisneros, M., & Baleanu, D. (2016).** Digital processing of thermographic images for medical applications. *Revista de Chimie*, Vol. 67, No. 1, pp. 53–56.
9. **Cheng, H.D., Cai, X., Chen, X., Hu, L., & Lou, X. (2003).** Computer-aided detection and classification of microcalcifications in mammograms: a survey. *Pattern Recognition*, Vol. 36, No. 12, pp. 2967–2991. DOI:10.1016/S0031-3203(03)00192-4.
10. **Kohonen, T. (1990)** The self organization map (SOM). *Proceedings of the IEEE*, Vol. 78, No. 9, pp.1464–1480.
11. **Mertzios, B.G. & Tsirikolias, K. (2001).** Applications of coordinate logic filters in image analysis and pattern recognition. *ISPA 2nd International Symposium on Image and Signal Processing and Analysis*, pp. 125–130. DOI: 10.1109/ISPA.2001.938615.
12. **Wirth, M., Fraschini, M., & Lyon, J. (2004).** Contrast enhancement of microcalcifications in mammograms using morphological enhancement and non-flat structuring elements. *17th IEEE Symposium on Computer-Based Medical System*, pp. 134–139. DOI: 10.1109/CBMS.2004.1311704.
13. **Gonzalez, R.C. & Woods, R.E. (2002).** *Digital image processing*. Prentice Hall.
14. **Ojeda-Magaña, B., Quintanilla-Domínguez, J., Ruelas, R., & Andina, D. (2009).** Images subsegmentation with the pfc clustering algorithm. *7th IEEE International Conference on Industrial Informatics*, pp. 499–503. DOI:10.1109/INDIN.2009.5195854.
15. **Bougioukos, P., Glotsos, D., Kostopoulos, S., Daskalakis, A., Kalatzis, I., Dimitropoulos, N., Nikiforidis, G., & Cavouras, D. (2010).** Fuzzy c-means-driven fhce contextual segmentation method for mammographic microcalcification detection. *The Imaging Science Journal*, Vol. 58, No. 3, pp. 146–154. DOI:10.1179/136821909X12581187860095.
16. **Andina, D., Álvarez-Vellisco, A., Jevtić, A., & Fombellida, J. (2009).** Artificial metaplasticity can improve artificial neural network learning. *In Intelligent Automation and Soft Computing*, Vol. 15, No. 4, pp. 681–694.
17. **Andina, D., Martinez-Antorrena, J., & Melgar, I. (2004).** Importance sampling in neural detector

- training phase. *Proceedings of World Automation Congress*, pp. 43–48.
18. **Fombellida, J., Torres-Alegre, S., Piñuela-Izquierdo, A.J., & Andina, D. (2015).** *Artificial Metaplasticity for Deep Learning: Application to WBCD Breast Cancer Database Classification*. Springer International Publishing, pp. 399–408. DOI: 10.1007/978-3-319-18833-1_42.
 19. **Richard, M.D. & Lippmann, R.P. (1991).** Neural network classifiers estimate bayesian a posteriori probabilities. *Neural computation*, Vol. 3, No. 4, pp. 461–483. DOI:10.1162/neco.1991.3.4.461.
 20. **Rojas, R. (1996).** A Short Proof of the Posterior Probability Property of Classifier Neural Networks. *Neural Computation*, Vol. 8, No. 1, pp. 41–43. DOI: 10.1162/neco.1996.8.1.41.
 21. **Fukunaga, K. (1990).** *Introduction to Statistical Pattern Recognition*. Academic Press, 2nd edition,
 22. **Marcano-Cedeño, A., Quintanilla-Domínguez, J., & Andina, D. (2009)** Wood defects classification using artificial metaplasticity neural network. *35th Annual Conference of the IEEE Industrial Electronics Society, IECON*, pp. 3422–3427. DOI: 10.1109/IECON.2009.5415189.
- Article received on 11/08/2016; accepted on 12/10/2016.
Corresponding author is Rafael Guzmán-Cabrera.